Environmental Science and Pollution Research (2019) 26:17548–17554
https://doi.org/10.1007/s11356-019-05099-w

RESEARCH ARTICLE

Microwave synthesis of ZnO nanoparticles using longan seeds biowaste and their efficiencies in photocatalytic decolorization of organic dyes

Chaiyos Chankaew[1] · Weerinradah Tapala[2] · Kate Grudpan[1] · Apinpus Rujiwatra[1]

Received: 26 November 2018 / Accepted: 4 April 2019 / Published online: 25 April 2019

Abstract

Crude water extract of the ground longan seeds which have been disposed in a large amount annually in Northern Thailand has been used in a simple and rapid microwave synthesis of ZnO nanoparticles. The particles were characterized by the UV-vis spectroscopy, Fourier-transformed infrared spectroscopy, X-ray diffraction, electron diffraction, energy dispersive X-ray spectroscopy, and transmission electron microscopy and revealed to be pure hexagonal phase. Influences of zinc precursor in the extract, microwave power, and irradiation time on particle sizes were studied. The use of 800 W and 30 cycles of the microwave irradiation provided the ZnO particles of 10–100 nm in size with an active surface area, a band gap energy, and a zero-point charge of 35 $m^2 \cdot g^{-1}$, 3.42 eV, and pH 7.7, respectively, after the calcination. Photocatalytic efficiencies of the synthesized particles were evaluated through the decolorization of methylene blue, malachite green, methyl orange, and orange II, and proved to be on par with commercially available titanium dioxide (Arroxide®P-25) under the same conditions. The use of the longan seeds biowaste as a sustainable supply of natural reagents for the green synthesis of ZnO nanoparticles which can be employed further for waste water treatment of the local textile dyeing industry is therefore presented.

Keywords Biowaste · Microwave synthesis · Zinc oxide · Nanoparticle · Photocatalyst

Introduction

The dried pulp of longan (*Dimocarpus longan* Lour.), which is also known as lumyai for the locals and dragon's eye for the Chinese, is one of the geographical indicators of Northern Thailand with high economic value. In the production of the dried longan pulp, a large amount of seeds is inevitably and continually disposed leading to environmental and hygienic problems for the locals as they attract flies and have become source of pathogens. To solve the emerging problems, the utilization of the longan seeds have been encouraged. Amidst various possibilities, the use of longan seeds as a supply of natural reagents for the green synthesis of ZnO photocatalyst is appealing since the wastewater pollution introduced from the textile dyeing industry is also prominent in Northern Thailand. In addition, almost all phytochemicals extracted from plants including, for instance, flavonoids, catechins, vitamins, proteins, and sugars can be employed as either the reducing or the capping agents, or both, in the synthesis of metal and metal oxide nanoparticles (Hebbalalu et al. 2013; Nadagouda et al. 2014; Nadagouda and Varma 2008; Varma 2012). Efficiency of the synthesis using these natural reagents can also be enhanced with the use of microwave heating (Baruwati et al. 2009; Baruwati and Varma 2009; Kou and Varma 2012a, 2012b), which also raises the feasibility of further development toward practical implementation (Kharissova et al. 2013).

The employment of the crude water extract of the ground longan seeds in the microwave synthesis of ZnO nanoparticles has been attempted. While the reason for the synthesis of ZnO lies in its nonhazardous properties according to the U.S. Food and Drug Administration (21CFR182.8991) (FDA 2011),

Responsible editor: Philippe Garrigues

✉ Apinpus Rujiwatra
apinpus.rujiwatra@cmu.ac.th

[1] Department of Chemistry, Faculty of Science, Chiang Mai University, 239 Houy Kaew Road, Moung, Chiang Mai 50200, Thailand

[2] Department of Chemistry, Faculty of Science, Maejo University, Chiang Mai 50290, Thailand

polyphenolic acids in the extract of the longan seeds (Soong and Barlow 2005; Sudjaroen et al. 2012) should be effective reagents in the synthesis. The presence of the polar functional groups in the structures of these phytochemicals (Fig. 1), among which the gallic and the ellagic acids are the major components, should additionally enhance the microwave heating in similar fashion to, for instance, glycerol and hydroxylated glycosides (Kou et al. 2013; Kou and Varma 2013). The biowaste would serve as a sustainable supply for the synthesis. Influences of important synthesis parameters on the formation of ZnO and the yielded particle sizes are presented. Performance of the synthesized ZnO nanoparticles in photocatalyzed decolorization of methylene blue (MB), malachite green (MG), methyl orange (MO), and orange II (OII), all of which have been used extensively by the local textile dyeing industry, was also evaluated in comparison with the commercialized TiO_2 (Arroxide®P-25).

Experimental

Synthesis and characterization of ZnO nanoparticles

Longan fruits of Edor cultivar were harvested from Pa Sang area, Lamphun Province, Thailand (18° 31′ 33″ N 98° 56′ 21″ E). The seeds were separated from peels and pulps right after the harvesting and were washed and dried at 75 °C for 24 before being ground to dark brown fine powder using a hammer mill (Armfield Hammer Mill FT2-A). The powder was stored in dark containers and kept at ca. 4 °C for further used throughout the project. The crude water extract of the powder was freshly prepared before each experiment using the procedure reported in the literature (Rangkadilok et al. 2007).

As a typical procedure (Somsri et al. 2016), Zn $(CH_3COO)_2{\cdot}2H_2O$ (≥ 99.0%, Aldrich) was dissolved in

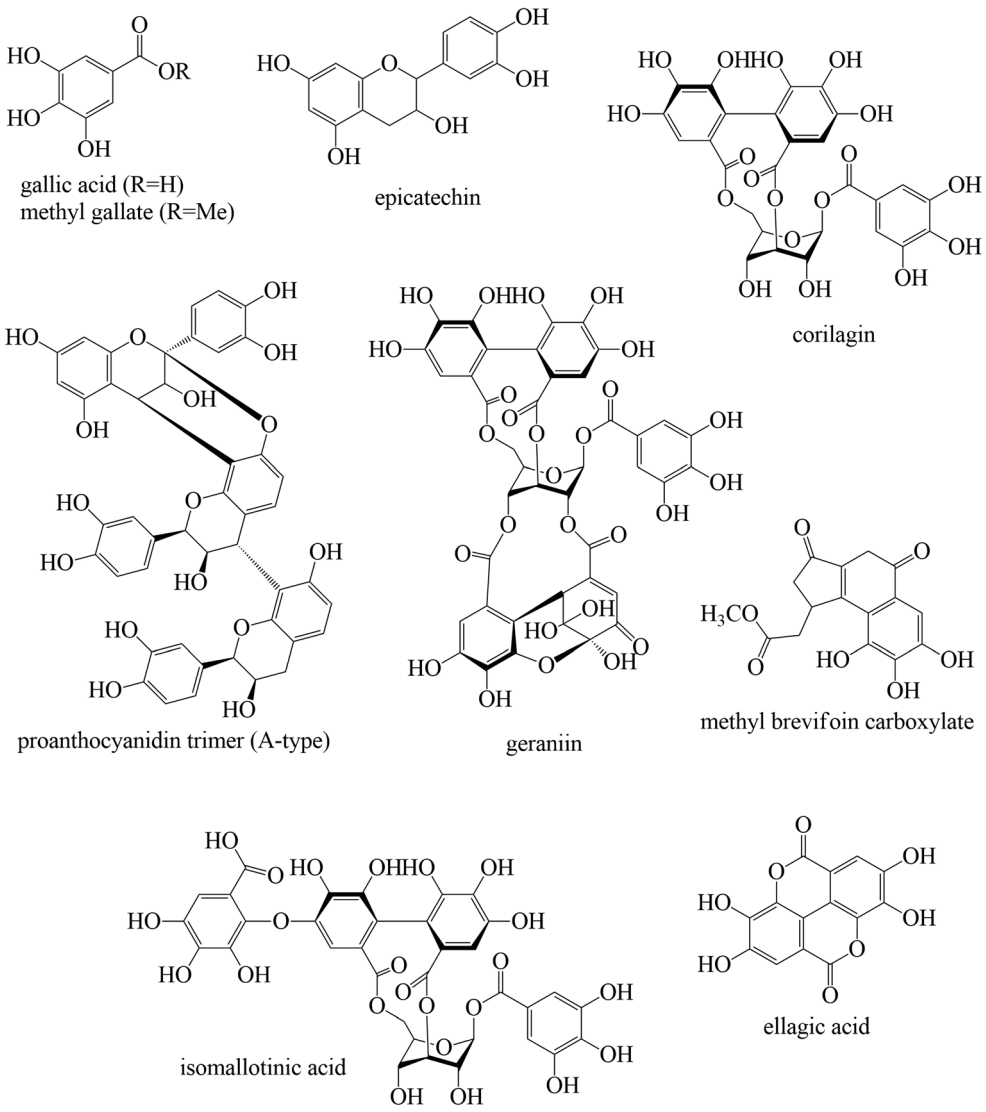

Fig. 1 Molecular structures of phytochemicals found in crude water extract of ground Edor longan seeds

10.00 mL of the extract to varying concentrations, i.e., 0.010 to 10.00 g·L^{-1}. The reaction was performed using a household microwave oven (Samsung Model MS23F301E), which was operated at various powers (450–800 W) and numbers of 1 min-on-1 min-off irradiation cycle (1–30 cycles). UV-vis spectroscopy (Shimadzu UV-1800) was employed to follow the synthesis reaction. The synthesized samples were characterized by the powder X-ray diffraction (PXRD; Bruker D8 Advance, Cu K_{α}, $\lambda = 1.54$ Å), the FT-IR spectroscopy (Bruker Tensor 27), and transmission electron microscopy (TEM; FEI TECNAI G2 20S-twin microscope1) equipped with selected area electron diffraction (SAED), the thermogravimetric analysis (TGA; NETZSCH STA 409 PC/PG), and the BrunauerEmmettTeller experiments (BET; Micromeritics/ASAP2460) conducted at 77 K with a prior degas at 300 °C for 12 h.

Photocatalytic dye decolorization experiments

Photocatalytic activities were evaluated from photocatalyzed decolorization of methylene blue (MB), malachite green (MG), methyl orange (MO), and orange II (OII). As a general procedure, 0.0240 g of the ZnO nanoparticles were suspended in 100.0 mL of 0.0160 g·L^{-1} dye solution. After leaving in the dark for 30 min, the reaction was exposed to artificial daylight (VeriVide F20 T12/D65 18 W, 300–830 nm), which was positioned at 12 cm above the suspension surface. An aliquot of 5.00 mL was taken from the reaction at every 15 min for the UV-vis spectroscopic measurement (Somsri et al. 2016). With reference to the calibration curve method, concentrations of the remaining dyes were determined. Compared with the initial concentration, efficiencies of the decolorization process were then calculated based on the reduced dye-concentration compared with the initial (Cai et al. 2017; Thennarasu et al. 2012). Photocatalytic decolorization of MB was additionally performed using different amounts of the ZnO nanoparticles ranging from 0.0100 to 0.3000 g. For comparison, Arroxide®P-25 (≥ 99.5%, Aldrich; particle size 21 nm, 36–65 m^2·g^{-1}; pHzpc = 7.5) and the as-synthesized samples were tested under the same experimental conditions.

Results and discussion

Microwave synthesis and ZnO nanoparticles

Based on characteristic absorptions of ZnO (Fig. 2), its formation was insignificant when the Zn $(CH_3COO)_2 \cdot 2H_2O$ concentration in the extract was lower than 1.00 g·L^{-1}, at which the characteristic absorption first appeared at the λ_{max} of 280 nm. As the precursor concentration was increased, this absorption feature became broadened with a small shoulder at 400 nm, suggesting a wide range of particle size distribution. The effect grew substantial when the precursor concentration was 10.0 g·L^{-1}, at which the multi-λ_{max} feature was apparent. An excessive concentration of the precursor in the extract is therefore detrimental to particle size homogeneity which should attribute to the particle growth. A severe diversity in the yielded particle size observed at 10.00 g·L^{-1} turned, however, silent when either the applied microwave power was ≤ 600 W or the irradiation cycle was ≤ 10 cycles.

The phytochemicals in the as-synthesized samples, denoted as ZnO^{amor} henceforth was manifested through the samples' chestnut-brown color, which was affirmed by the FT-IR spectra of the yielded samples compared with the dried extract (Fig. 3). The primary vibrational features, including ν (O-H; 2985–3670 cm^{-1}), ν (C=O; 1585 cm^{-1}), ν (C-OH; 1415 cm^{-1}), and δ (C-OH; 1041 cm^{-1}), correspond well to the functional groups of the phytochemicals found in the extract among which gallic and ellagic acids are the major components (De Goes Sampaio et al. 2019; Sudjaroen et al. 2012). The capping phytochemicals were also explicit in the TEM images showing the expansive light area of the phytochemicals and the dark areas of the ZnO^{amor} (Fig. 4). The PXRD patterns collected on these powders suggested them to be amorphous, which is not unexpected as the long-range structural order of the derived ZnO^{amor} should be disrupted by the capping phytochemicals.

Upon the heating of the ZnO^{amor} from room temperature to 900 °C under the nitrogen gas flow (Fig. 3), a gradual weight loss of over 70% occurred resulting in a white powder. The temperature at which the significant weight loss commenced is in a typical range where the organic molecules in most coordination compounds decompose. This is well supported by the FT-IR spectrum of the white powder, exhibiting only ν (Zn-O) at 440 cm^{-1} and the ν (O-H) of possibly the surface water centering at 3418 cm^{-1} (Nosrati et al. 2012; Wu et al. 2016). The complete removal of the capping phytochemicals by a simple heat treatment can therefore be assumed, which is ascertained by the TEM images displaying only the well-defined ZnO (Fig. 4). This can be regarded as one of the merits of the longan seeds extract since the complete removal of the capping phytochemicals to generate an active surface of the ZnO nanoparticles is the inherent drawback of the phytosynthesis process. The remaining of the phytochemicals can obstruct access to the surface of the particles and nullify their activity (Somsri et al. 2016).

The yielded white powder was characterized to be a pure phase of hexagonal ZnO (JCPDS 36–1451; $a = 3.247(8)$ Å, $c = 5.202(6)$ Å) by the PXRD (Fig. 3) and the SAED (Fig. 4) experiments. The heat treatment can thereby be regarded also as the calcination step. According to the TEM images, shapes of the ZnO particles were mostly irregular although some

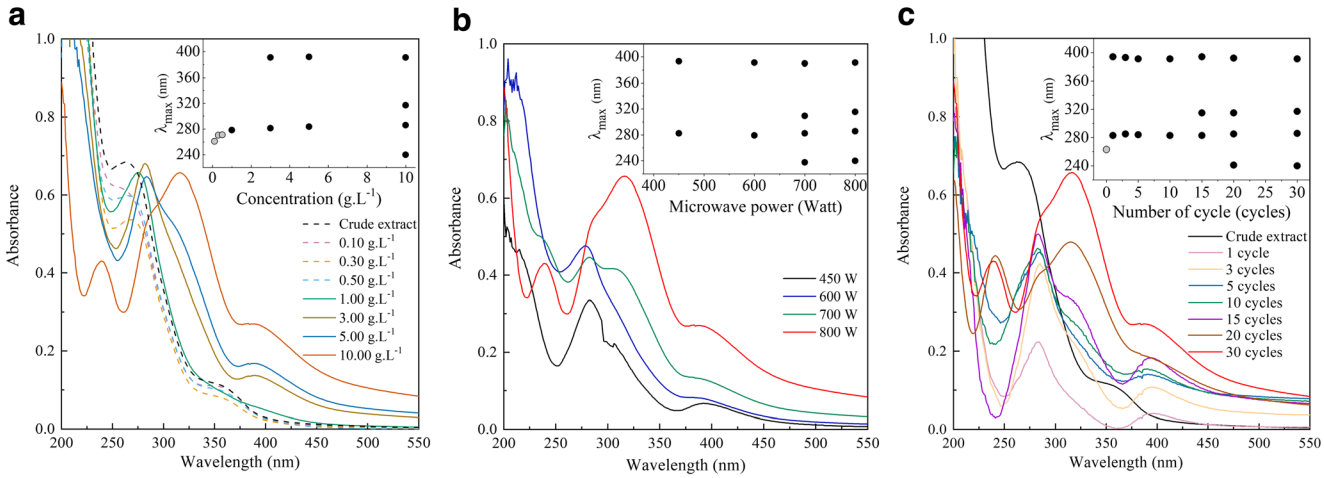

Fig. 2 UV-vis spectra of the reaction mixtures under the following conditions: **a** varied precursor concentration, 800 W, 30 cycles; **b** varied microwave power, 30 cycles, 10.0 g L^{-1} precursor; and **c** varied number of irradiation cycles, 800 W, 10.0 g·L^{-1} precursor, with the corresponding λ_{max} in the inset (● = extract, ●= ZnO)

clearly manifested the inherent hexagonal symmetry. Sizes of the particles were distributed from 10 to 100 nm of which 50% and 78% were in the ranges of 40–60 nm and 40–80 nm, respectively (Fig. 4). The BET surface area of these ZnO nanoparticles was found to be 35 $m^2 \cdot g^{-1}$. The band gap energy of 3.42 eV was determined from the Kubelka-Munk plot and is in the common range reported for the ZnO nanoparticles (Cai et al. 2017; Janotti and Van de Walle 2009; Reynolds et al. 1999; Srikant and Clarke 1998).

Photocatalytic activities of ZnO nanoparticles in decolorization of organic dyes

In accordance with the decolorization of the cationic MB and MG, and the anionic MO and OII, performances of the ZnO nanoparticles and the commercially available TiO_2 (Arroxide®P-25) were approximately on par (Fig. 5 and Fig. 6). Efficiency of the ZnO nanoparticles was substantial in the case of MB of which over 70% of the dye was decolored in only half an hour and almost 100% in approximately an hour. The particles became, however, less efficient for the decolorization of MG, OII, and MO, successively. Such disparity can be accounted for by different accessibility of these dyes onto the surface of the ZnO nanoparticles, which is well acknowledged as being crucial in determining efficiency of the catalyst (Abdel-Khalek et al. 2018; Thirumavalavan et al. 2013). The assumption is supported by the silent activities of the chestnut-brown ZnO^{amor} where the access to the nanoparticles' surface should be blocked by the capping phytochemicals.

Accessibility onto the surface of the photocatalyst depends however on the surface charge of the organic dyes at the experimental pH. Based on the pH drift method (Intarasuwan et al. 2017), the pH at the zero-point charge (pHzpc) estimated

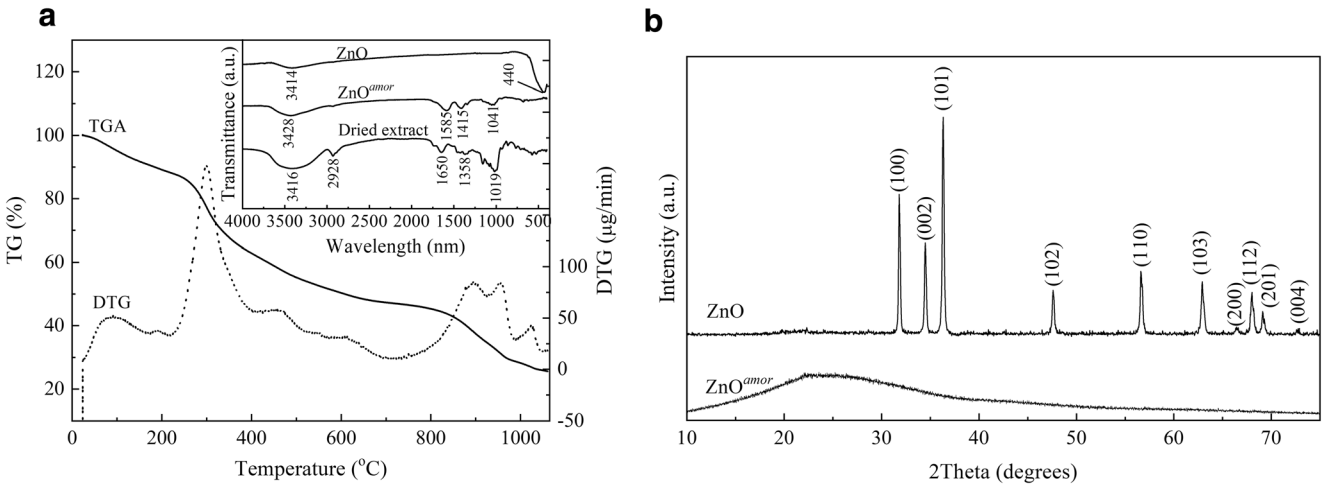

Fig. 3 **a** TGA diagram of ZnO^{amor} with the FT-IR spectra (inset) of the dried extract compared with ZnO^{amor} and ZnO, and **b** the PXRD patterns of ZnO^{amor} and ZnO

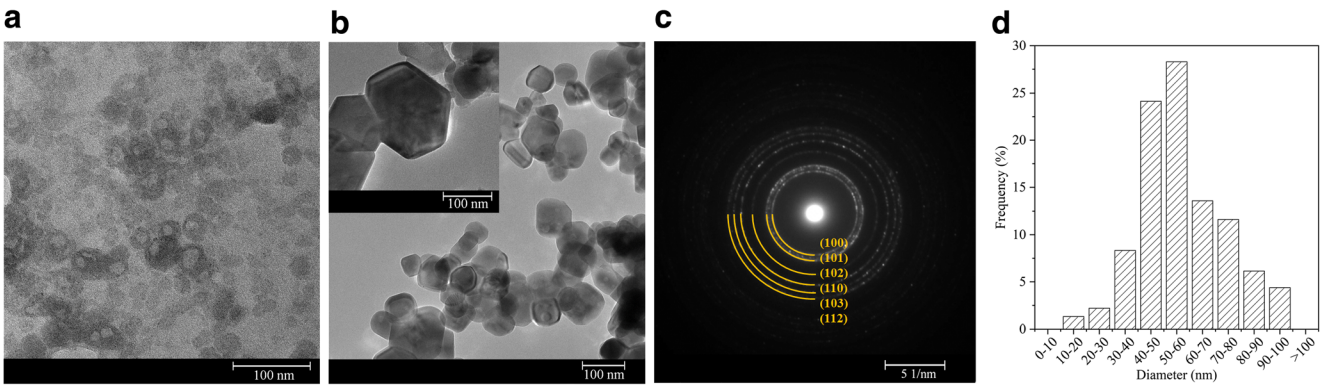

Fig. 4 TEM images of **a** ZnO^{amor} and **b** ZnO, with the corresponding **c** SAED pattern and **d** particle size distribution of ZnO

for the yielded ZnO nanoparticles was 7.7. Compared with the pH at which the experiments were performed (pH = 8.5), the negatively charged surface could be assumed for the ZnO. The preference toward the adsorption of the cationic dyes (MB and MG) and better catalytic efficiency than the negative dyes (MO and OII) can thus be accounted for by an electrostatic interaction. The better performance of the cationic MB bearing a positive charge at pH > 3.8 (Kim et al. 2013) than that of MG of which the pK_a is 6.9 (Culp and Beland 1996) can be rationalized by the feasible co-existence of both the cationic and the neutral carbinol forms of MG (Culp and Beland 1996; Cuong et al. 2012). In concert with the decolorization of MB (Fig. 5), the increase in amount of the ZnO nanoparticles has been revealed to shorten the reaction time required for the complete decolorization. The amount of the ZnO nanoparticles over 0.1000 g however did not introduce any improvement, suggesting the reaching of its limitation under the employed conditions.

Conclusions

In summary, the crude water extract of ground Edor longan seeds has been used in the facile and rapid microwave synthesis of ZnO nanoparticles although the calcination was required. The capping phytochemicals could be completely removed to activate the photocatalytic activity of the particles during the calcination, which can be regarded as the major merit of the longan seed extract. The use of 10.0 g·L^{-1} zinc acetate, 800 W, and 30 cycles of the microwave irradiation with successive heating at 900 °C for 1.5 h provided the pure hexagonal phase of ZnO nanoparticles of 10–100 nm in sizes and the BET surface area of 35 m^2·g^{-1}. At the pH of 8.5, the efficiencies of these ZnO nanoparticles (band gap energy = 3.42 eV and pHzpc = 7.7) toward the decolorization of some commonly used organic dyes were approximately on par with the commercially available TiO_2 (Arroxide®P-25). Based on

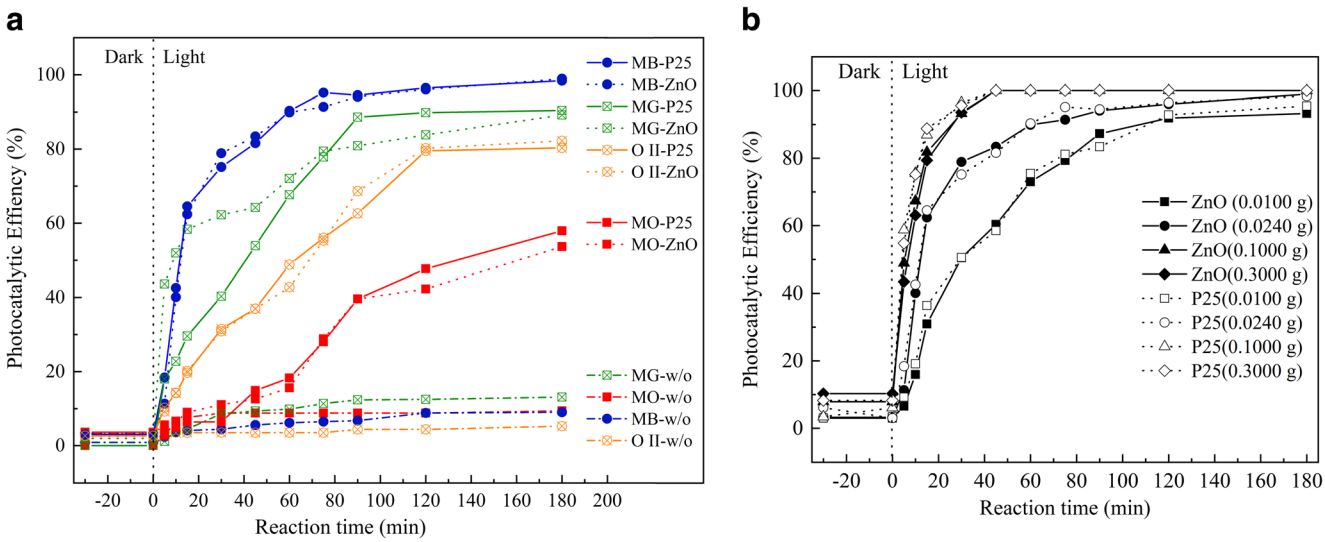

Fig. 5 Efficiencies of ZnO in photocatalyzed decolorization of **a** MB, MG, MO, and OII, compared with those of TiO_2 (Arroxide®P-25), and **b** of MB only but with different amounts of the catalysts

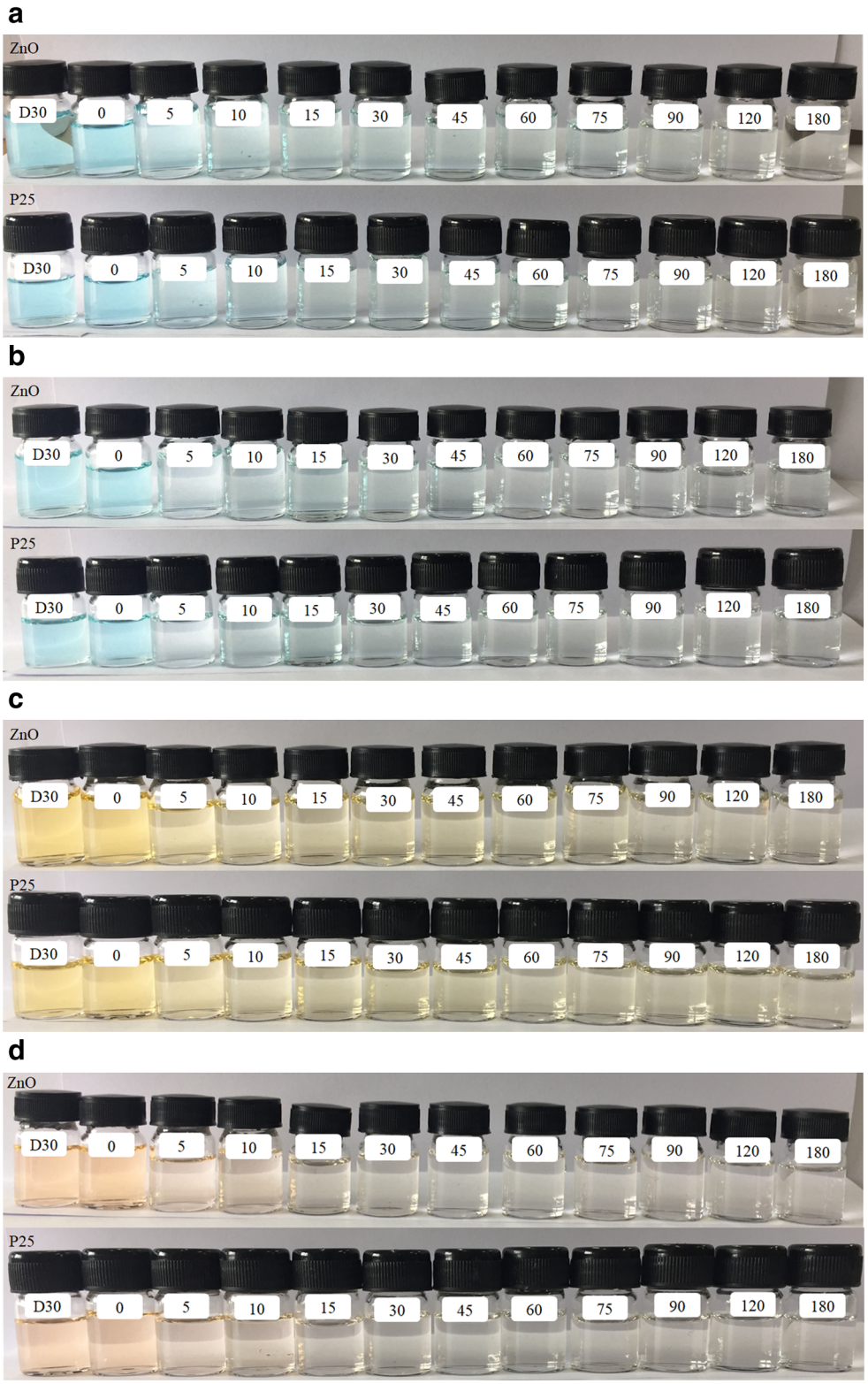

Fig. 6 Photos showing time-dependent decolorization of **a** MB, **b** MG, **c** MO, and **d** OII solutions catalyzed by ZnO (upper row) and TiO_2 (Arroxide®P-25; lower row)

this study, an alternative utilization of the longan seeds which are readily and sustainably available in Northern Thailand is demonstrated. The ZnO nanoparticles synthesized using the water extract of this biowaste can promisingly be employed in the treatment of wastewater released from the local textile dyeing industry.

Acknowledgements C. Chankaew thanks the Rajamangala University of Technology Isan and the Graduate School of Chiang Mai University for the graduate scholarships.

Funding information This work is funded by the TRF Distinguished Research Professor Award (DPG6080002) and the Higher Education Research Promotion of the Office of the Higher Education Commission.

References

Abdel-Khalek AA, Mahmoud SA, Zaki AH (2018) Visible light assisted photocatalytic degradation of crystal violet, bromophenol blue and eosin Y dyes using AgBr-ZnO nanocomposite. Environ Nanotechnol Monit Manag 9:164–173. https://doi.org/10.1016/j.enmm.2018.03.002

Baruwati B, Polshettiwar V, Varma RS (2009) Glutathione promoted expeditious green synthesis of silver nanoparticles in water using microwaves. Green Chem 11:926. https://doi.org/10.1039/b902184a

Baruwati B, Varma RS (2009) High value products from waste: grape pomace extract-a three-in-one package for the synthesis of metal nanoparticles. Chem Sus Chem 2:1041–1044. https://doi.org/10.1002/cssc.200900220

Cai Z, Sun Y, Liu W, Pan F, Sun P, Fu J (2017) An overview of nanomaterials applied for removing dyes from wastewater. Environ Sci Pollut Res 24:15882–15904. https://doi.org/10.1007/s11356-017-9003-8

Culp SJ, Beland FA (1996) Malachite green: a toxicological review. J Am Coll Toxicol 15:219–238. https://doi.org/10.3109/10915819609008715

De Goes Sampaio C, Silva JGAE, De Brito ES, Becker H, Trevisan MTS, Owen RW (2019) Chromium (VI) remediation in aqueous solution by waste products (peel and seed) of mango (*Mangifera indica L.*) cultivars. Environ Sci Pollut Res 26:5588–5600. https://doi.org/10.1007/s11356-018-3851-8

FDA (2011) Substances generally recognized as safe, in: Code of Federal Regulations Title 21 Food and Drug Administration: parts 170–199. U.S. Government Printing Office, Washington DC, USA. https://www.gpo.gov/fdsys/pkg/CFR-2011-title21-vol3/pdf/CFR-2011-title21-vol3.pdf. Accessed 16 May 2018

Hebbalalu D, Lalley J, Nadagouda MN, Varma RS (2013) Greener techniques for the synthesis of silver nanoparticles using plant extracts, enzymes, bacteria, biodegradable polymers, and microwaves. ACS Sustain Chem Eng 1:703–712. https://doi.org/10.1021/sc4000362

Intarasuwan K, Amornpitoksuk P, Suwanboon S, Graidist P (2017) Photocatalytic dye degradation by ZnO nanoparticles prepared from $X_2C_2O_4$ (X = H, Na and NH_4) and the cytotoxicity of the treated dye solutions. Sep Purif Technol 177:304–312. https://doi.org/10.1016/j.seppur.2016.12.040

Janotti A, Van de Walle CG (2009) Fundamentals of zinc oxide as a semiconductor. Rep Prog Phys 72:126501. https://doi.org/10.1088/0034-4885/72/12/126501

Kharissova OV, Dias HVR, Kharisov BI, Olvera Pérez B, Jiménez Pérez VM (2013) The greener synthesis of nanoparticles. Trends Biotechnol 31:240–248. https://doi.org/10.1016/j.tibtech.2013.01.003

Kim JR, Santiano B, Kim H, Kan E (2013) Heterogeneous oxidation of methylene blue with surface-modified iron-amended activated carbon. Am J Anal Chem 04:115–122. https://doi.org/10.4236/ajac.2013.47A016

Kou J, Bennett-Stamper C, Varma RS (2013) Green synthesis of noble nanometals (Au, Pt, Pd) using glycerol under microwave irradiation conditions. ACS Sustain Chem Eng 1:810–816. https://doi.org/10.1021/sc400007p

Kou J, Varma RS (2013) Speedy fabrication of diameter-controlled Ag nanowires using glycerol under microwave irradiation conditions. Chem Commun 49:692–694. https://doi.org/10.1039/C2CC37696B

Kou J, Varma RS (2012a) Beet juice utilization: expeditious green synthesis of noble metal nanoparticles (Ag, Au, Pt, and Pd) using microwaves. RSC Adv 2:10283–10290. https://doi.org/10.1039/c2ra21908e

Kou J, Varma RS (2012b) Beet juice-induced green fabrication of plasmonic AgCl/Ag nanoparticles. Chem Sus Chem 5:2435–2441. https://doi.org/10.1002/cssc.201200477

Cuong MN, Ishizaka S, Kitamura N (2012) Donnan electric potential dependence of intraparticle diffusion of malachite green in single cation exchange resin particles: a laser trapping-microspectroscopy study. Am J Anal Chem 03:188–194. https://doi.org/10.4236/ajac.2012.33027

Nadagouda MN, Iyanna N, Lalley J, Han C, Dionysiou DD, Varma RS (2014) Synthesis of silver and gold nanoparticles using antioxidants from blackberry, blueberry, pomegranate, and turmeric extracts. ACS Sustain Chem Eng 2:1717–1723. https://doi.org/10.1021/sc500237k

Nadagouda MN, Varma RS (2008) Green synthesis of silver and palladium nanoparticles at room temperature using coffee and tea extract. Green Chem 10:859–862. https://doi.org/10.1039/b804703k

Nosrati R, Olad A, Maramifar R (2012) Degradation of ampicillin antibiotic in aqueous solution by ZnO/polyaniline nanocomposite as photocatalyst under sunlight irradiation. Environ Sci Pollut Res 19:2291–2299. https://doi.org/10.1007/s11356-011-0736-5

Rangkadilok N, Sitthimonchai S, Worasuttayangkurn L, Mahidol C, Ruchirawat M, Satayavivad J (2007) Evaluation of free radical scavenging and antityrosinase activities of standardized longan fruit extract. Food Chem Toxicol 45:328–336. https://doi.org/10.1016/J.fct.2006.08.022

Reynolds DC, Look DC, Jogai B, Litton CW, Cantwell G, Harsch WC (1999) Valence-band ordering in ZnO. Phys Rev B 60:2340–2344. https://doi.org/10.1103/Physrevb.60.2340

Somsri S, Sonwaew W, Rujiwatra A (2016) *Psidium guajava* Linn. extract mediated microwave synthesis and photocatalytic activities of ZnO nanoparticles. Mater Lett 177:124–127. https://doi.org/10.1016/j.matlet.2016.04.130

Soong YY, Barlow PJ (2005) Isolation and structure elucidation of phenolic compounds from longan (*Dimocarpus longan* Lour.) seed by high-performance liquid chromatography–electrospray ionization mass spectrometry. J Chromatogr A 1085:270–277. https://doi.org/10.1016/j.chroma.2005.06.042

Srikant V, Clarke DR (1998) On the optical band gap of zinc oxide. J Appl Phys 83:5447–5451. https://doi.org/10.1063/1.367375

Sudjaroen Y, Hull WE, Erben G, Würtele G, Changbumrung S, Ulrich CM, Owen RW (2012) Isolation and characterization of ellagitannins as the major polyphenolic components of Longan (*Dimocarpus longan* Lour) seeds. Phytochemistry 77:226–237. https://doi.org/10.1016/j.phytochem.2011.12.008

Thennarasu G, Kavithaa S, Sivasamy A (2012) Photocatalytic degradation of Orange G dye under solar light using nanocrystalline semiconductor metal oxide. Environ Sci Pollut Res 19:2755–2765. https://doi.org/10.1007/s11356-012-0775-6

Thirumavalavan M, Yang FM, Lee JF (2013) Investigation of preparation conditions and photocatalytic efficiency of nano ZnO using different polysaccharides. Environ Sci Pollut Res 20:5654–5664. https://doi.org/10.1007/s11356-013-1575-3

Varma RS (2012) Greener approach to nanomaterials and their sustainable applications. Curr Opin Chem Eng 1:123–128. https://doi.org/10.1016/J.COCHE.2011.12.002

Wu L, Zhang Y, Yang G, Zhang S, Yu L, Zhang P (2016) Tribological properties of oleic acid-modified zinc oxide nanoparticles as the lubricant additive in poly-alpha olefin and diisooctyl sebacate base oils. RSC Adv 6:69836–69844. https://doi.org/10.1039/C6RA10042B